

Learning noise via dynamical decoupling of entangled qubitsTrevor McCourt,^{1,2} Charles Neill,³ Kenny Lee ³, Chris Quintana,³ Yu Chen,³ Julian Kelly,³ Jeffrey Marshall ^{4,5}, V. N. Smelyanskiy,³ M. I. Dykman ⁶, Alexander Korotkov,³ Isaac L. Chuang,^{1,7} and A. G. Petukhov³¹*Department of Electrical Engineering and Computer Science, Massachusetts Institute of Technology, Cambridge, Massachusetts 02139, USA*²*Department of Physics, Co-Design Center for Quantum Advantage, Massachusetts Institute of Technology, Cambridge, Massachusetts 02139, USA*³*Google Quantum AI, Santa Barbara, California 93101, USA*⁴*QuAIL, NASA Ames Research Center, Moffett Field, California 94035, USA*⁵*USRA Research Institute for Advanced Computer Science, Mountain View, California 94043, USA*⁶*Department of Physics and Astronomy, Michigan State University, East Lansing, Michigan 48824, USA*⁷*Department of Physics, Massachusetts Institute of Technology, Cambridge, Massachusetts 02139, USA*

(Received 15 February 2022; accepted 8 May 2023; published 22 May 2023)

Understanding noise in entangled systems is a prerequisite for developing scalable quantum computers. Here, we propose and apply multiqubit dynamical decoupling sequences that characterize noise during two-qubit gates. This noise is qualitatively different from the well-studied noise that leads to single-qubit dephasing; it simultaneously affects the two qubits, inducing fluctuations in their entangling parameter. In our superconducting system, the experimentally observed noise comes from coupler flux fluctuations and is observed to be non-Gaussian, leading to the stepwise decay of signals.

DOI: [10.1103/PhysRevA.107.052610](https://doi.org/10.1103/PhysRevA.107.052610)**I. INTRODUCTION**

Producing interesting, large-scale quantum dynamics in engineered systems is being made increasingly possible by the advancement of superconducting qubits. Transmon qubits that use frequency tunable couplers to realize interqubit interactions have been successful at this task in the areas of quantum simulation [1–3], quantum chemistry [4], and theoretical computer science [5–8]. Imperative to this is the ability to generate entanglement using high-fidelity two-qubit gates [9,10]. As control of these gates is improved, their performance will start to become limited by a system-environment interaction. The characterization and eventual mitigation of this noise producing interaction is therefore critical to continual forward progress.

Traditionally, the bulk of low-frequency noise characterization in qubits has been dedicated to the study of single-qubit dephasing noise. This is modeled as either a qubit coupling to external quantum degrees of freedom or as classical stochastic fluctuations in the qubit frequency [11]. Most often, the noise is assumed to have Gaussian statistics. In this Gaussian scenario, sophisticated tools have been developed to characterize the power spectral density of the noise [12–15]. There have also been efforts to characterize noise outside of this regime. These have been focused on measuring the higher-order moments of single-qubit non-Gaussian dephasing [16,17] as well as characterizing spatially correlated Gaussian dephasing noise [18–20].

Studies of single-qubit dephasing may be sufficient to understand the behavior of small systems involving only one or a few qubits. However, large systems have many degrees of freedom, and therefore many channels through which noise can enter. For example, noise that occurs during

two-qubit gates may lead to noise that affects two qubits simultaneously. Understanding these two-qubit noise mechanisms in the context of quantum computing will be important for implementing near term quantum algorithms and building a fault-tolerant quantum computer in the long term. Indeed, recent work has begun to develop methods for characterizing multiqubit noise [21,22]. Experimentally, the difficulty in characterizing noise in larger systems stems from the fact that measurement of a particular kind of noise may be confounded by competing error mechanisms, as larger systems are generally more difficult to control precisely than the small ones.

In this paper, we characterize noise that occurs during two-qubit gates. The gate we study is performed using a tunable coupler that modulates the qubit-qubit coupling. Our key observation is that the primary source of noise is frequency fluctuations of this coupler. These fluctuations lead to noise in the entangling parameter g , the coupling strength between the two qubits. The noise is therefore turned on during a gate operation and affects two qubits simultaneously, in qualitative distinction from single-qubit dephasing. We show that this fundamentally two-qubit noise can be studied by driving pairs of qubits through two-qubit pulse sequences with interleaved coupler and qubit frequency control. We find that in many samples this noise is composed of Gaussian $1/f$ noise, similar to the noise dominating single-qubit dephasing, and a signal from a few random telegraph fluctuators. These findings are significant because both the two-qubit and non-Gaussian nature of the observed noise may require new error mitigation techniques [23]. Additionally, the clean signatures of non-Gaussian noise that we see are a significant departure from what is typically assumed and observed in condensed matter systems, where Gaussian $1/f$ noise is ubiquitous [24–27].

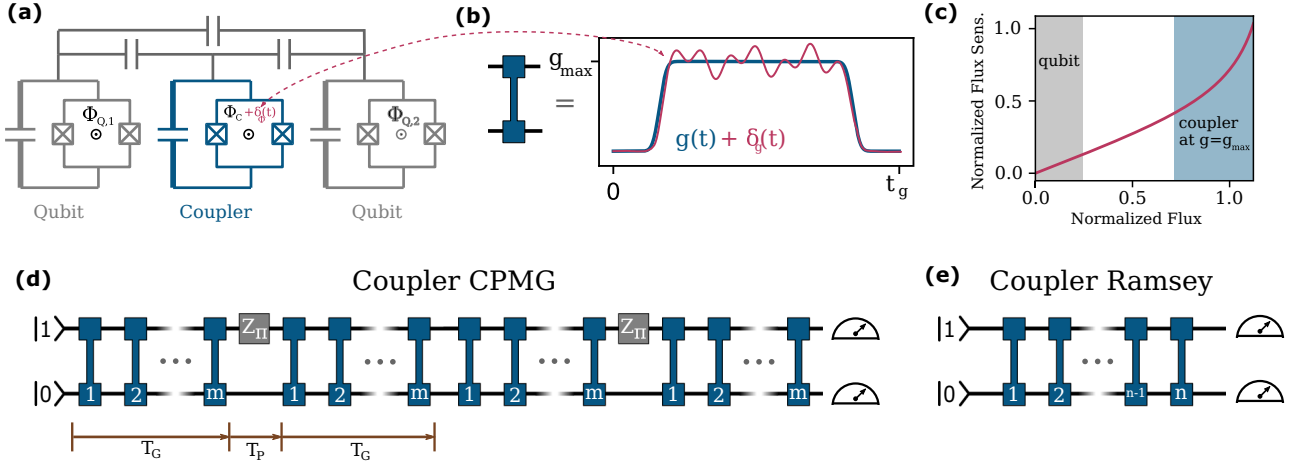


FIG. 1. Circuits for entangled noise metrology. (a) Simplified circuit diagram for two qubits and the tunable coupler. The qubit frequencies ω_j are modulated by changing $\Phi_{Q,j}$. The coupler frequency is changed significantly during two-qubit gates via Φ_c . (b) Schematic of the time-dependent coupling $g(t)$ enacted during two-qubit gates. The coupler flux noise $\delta_\phi(t)$ generates coupling fluctuations $\delta_g(t)$ according to Eq. (4). (c) Flux sensitivity χ [Eq. (5)] vs external flux. The qubits are generally operated at frequencies with much lower flux sensitivity than the coupler. (d) Circuit diagram showing the coupler Carr-Purcell-Meiboom-Gill (CPMG) sequence. Shown here are $n = 2$ repetitions of a pulse sequence involving $2m$ two-qubit gates that are separated by a qubit frequency π pulse. The two-qubit gates serve to expose the qubits to g noise, which is refocused by the frequency pulse. The decay of the pseudoqubit (σ_z) observable is measured at the end of the circuit, which can be used to characterize the noise. See Supplemental Material Sec. L [28] for further examples. (e) Circuit diagram showing the coupler Ramsey sequence involving n two-qubit gates, which can be used to measure the response of the qubits to g noise in the absence of refocusing pulses.

We begin by introducing the theory of flux noise entering through the coupler and a technique for measuring it. We then present the measurement results and show that while they match well what would be expected for coupler flux noise, they do not agree well with Gaussian theory. Finally, we generalize to a non-Gaussian model of the noise and validate it with further experiments.

II. FLUX NOISE IN THE COUPLER

The single excitation subspace of two qubits is spanned by the states $|01\rangle$ and $|10\rangle$ and forms a pseudoqubit with the Hamiltonian

$$H = \frac{1}{2}[\omega(t) + \delta\omega(t)]\sigma_z + [g(t) + \delta g(t)]\sigma_x, \quad (1)$$

where $\sigma_z = |01\rangle\langle 01| - |10\rangle\langle 10|$ and $\sigma_x = |01\rangle\langle 10| + |10\rangle\langle 01|$. Here, $\omega(t)$ and $\delta\omega(t)$ are the control and noise contributions to the difference of the qubit frequencies, respectively, while $g(t)$ and $\delta g(t)$ are the control and noise contributions to the interqubit coupling.

During many types of two-qubit gates, the two qubits are on resonance, $\omega(t) = 0$. In this case, $\delta\omega(t)$ and $g(t) + \delta g(t)$ can be considered respectively as z and x components of an effective magnetic field. The Bloch vector of our effective two-level system undergoes Larmor precession around the instantaneous axis, which is almost parallel to the x field, with the instantaneous Larmor frequency given by

$$\omega_L(t) \simeq 2g(t) + 2\delta g(t) + \frac{\delta\omega^2(t)}{4g(t)}. \quad (2)$$

From this, we can see that coupler noise will dominate during these resonant two-qubit gates: $\delta g(t)$ shows up to first

order in the dynamics while $\delta\omega(t)$ only shows up to second order and is suppressed by a factor of $g(t)$.

Coupler noise physically results from coupler frequency fluctuations. In our tunable coupler system depicted in Fig. 1, the qubit frequencies ω_q and the coupler frequencies ω_c are controllable via the external fluxes, Φ_q and Φ_c , respectively and the relation between ω and Φ is $\omega \simeq \omega_{\max} \sqrt{|\cos(\frac{\pi\Phi}{\Phi_0})|}$, where Φ_0 is the flux quantum. The coupling g developed between two qubits that are on resonance at ω_q is given by [29]

$$g \simeq \left(k_d - k^2 \frac{\omega_q^2}{\omega_c^2 - \omega_q^2} \right) \frac{\omega_q}{2}, \quad (3)$$

where k and k_d are the indirect and direct coupling efficiencies that are functions of circuit parameters (see Supplemental Material Sec. C [28]). The pseudoqubit defined in Eq. (1) is therefore completely controllable via low-frequency manipulation of the qubit and coupler flux biases and no microwave control is necessary to implement dynamical decoupling of the entangled qubits. Another characteristic feature of our method is its use of excitation preserving dynamics, which allow us to separate the effects of qubit decay from the desired signal.

Fluctuations in Φ lead to fluctuations in frequency, i.e., to flux noise, which is ubiquitous in superconducting quantum interference devices (SQUIDs) [30]. During gates, the sensitivity of the coupler frequency to flux noise is substantially larger than that of the qubit [see Fig. 1(b)]. Noise in the coupler frequency leads to fluctuations in g . The fluctuation $\delta g(t)$ in the Hamiltonian (1) can be expressed through coupler

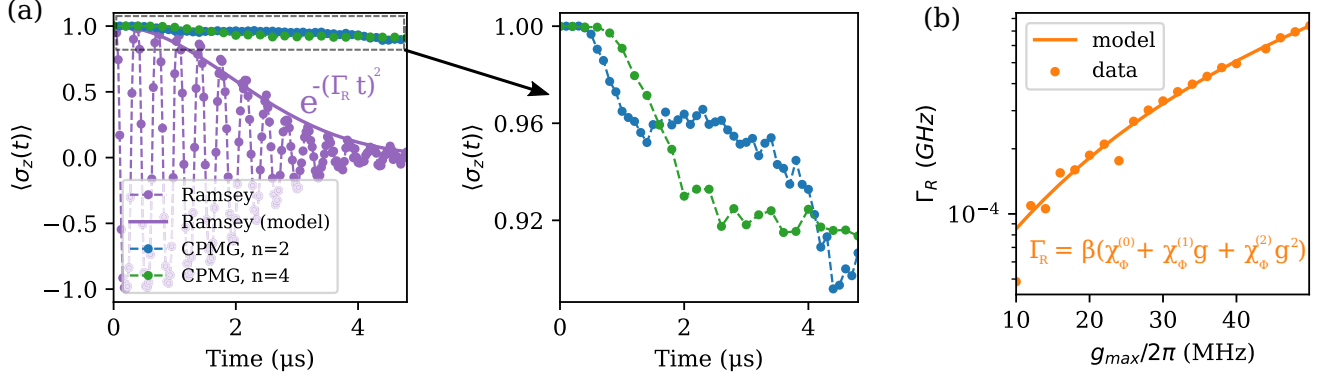


FIG. 2. Experimentally observed Ramsey and CPMG dynamics. (a) Comparing coupler Ramsey decay of normalized population difference [Eq. (8)] with $g_{\text{max}} = 30$ MHz to decay under $n = 2$ and $n = 4$ coupler CPMG sequences. The x axis is total evolution time, $t = nt_g$ for Ramsey and $t = 2mnt_g$ for CPMG. The duration of a fixed n CPMG sequence is modified by changing m . We see that the CPMG sequences effectively mitigate most of the decoherence, suggesting that most of the noise power is at low frequencies. The Gaussian shape of the Ramsey decay envelope is typical of $1/f$ -type noise [see Eq. (6)]. When observed in detail, the CPMG decay envelopes display behavior not predicted by Gaussian theory. Increasing the number of CPMG pulses does not increase noise protection as predicted by Eq. (7); the curves braid and have steps. All data points are the average of 10 000 samples. (b) Ramsey decay rate Γ_R vs g_{max} . We see that the decay rate is strongly dependent on g_{max} , crossing an order of magnitude in 30 MHz. The g_{max} dependence is well predicted by Eq. (4) given typical circuit parameters.

flux fluctuations $\delta\Phi_c(t)$ as follows,

$$\delta g(t) = 2\pi \tilde{\chi}_\phi(g) \delta\Phi_c(t) = \lambda(g) \xi(t), \quad (4)$$

where the flux sensitivity of g is defined as

$$\tilde{\chi}_\phi = \frac{1}{2\pi} \left| \frac{dg}{d\Phi_c} \right| \simeq \chi_\phi^{(0)} + \chi_\phi^{(1)}g + \chi_\phi^{(2)}g^2. \quad (5)$$

Here, $\xi(t)$ is a dimensionless classical random variable modeling flux fluctuations with characteristic amplitude $\delta\Phi_m$, and $\lambda(g) = 2\pi \tilde{\chi}_\phi(g) \delta\Phi_m$ is the amplitude of g noise. It can be shown (see Supplemental Material Sec. C [28]) that in the studied parameter range the quadratic dependence of $\tilde{\chi}_\phi(g)$, displayed in Eq. (5), follows directly from Eq. (3).

III. NOISE METROLOGY TECHNIQUE

The effect of g noise on the pseudoqubit defined in Eq. (1) may be characterized using what we call the coupler Carr-Purcell-Meiboom-Gill (CPMG) pulse sequence. In this sequence, the pseudoqubit is initialized in the state $|01\rangle$ via a microwave pulse. It is then exposed to n repetitions of a spin-echo-like pulse sequence [31], each of which consists of a fast π rotation around the z axis ($\sigma_z \pi$ pulse) buffered before and after by exposure to g noise for time T_G . The σ_z pulse has the effect of refocusing the $\sigma_x g$ noise. This exposure to g noise is accomplished by m repetitions of a Floquet-calibrated [1] two-qubit gate with duration t_g for which $\omega = 0$ and $|g| > 0$ [see Fig. 1(b)]. There are a total of $2m$ two-qubit gates between refocusing pulses; the total time between refocusing pulses is therefore $2mt_g$. After the n echo sequences are completed, we can measure the pseudoqubit observable $\langle \sigma_z \rangle$, which will decay due to g noise. Studying the decay of this observable will reveal the character of the noise. The coupler CPMG pulse sequence is shown in Fig. 1(d). This pulse sequence is analogous to standard, single-qubit CPMG [32,33], with the main difference being that it takes place in the z - y plane of the Bloch sphere instead of the x - y plane, so the direction of refocusing pulses and measurements must

be adjusted accordingly. It is also desirable to observe the σ_z decay due to g noise in the absence of the refocusing pulses. This may be done using the coupler Ramsey pulse sequence see [Fig. 1(e)].

The statistics of $\xi(t)$ dictate what type of decay we expect to see during these sequences. A common assumption is $\xi(t)$ is a Gaussian random process with a $1/f$ power spectrum. In this case, for decay under the coupler Ramsey sequence we would expect (up to logarithmic corrections, see Supplemental Material Sec. G [28])

$$\langle \sigma_z(t) \rangle \simeq e^{-(\Gamma_R t)^2} \cos(Gt), \quad \Gamma_R \propto \lambda, \quad (6)$$

where G is the coherent swap frequency. In the case of decay under an n -pulse CPMG sequence,

$$\langle \sigma_z(t) \rangle \simeq e^{-(\Gamma_C t)^2}, \quad \Gamma_C \propto \frac{\lambda}{\sqrt{n}}. \quad (7)$$

We experimentally characterize g -noise on our superconducting qubit device [7] by executing these sequences. We measure the observable

$$\frac{\langle \sigma_z \rangle}{\langle I \rangle} = \frac{\langle 01 | \rho(t) | 01 \rangle - \langle 10 | \rho(t) | 10 \rangle}{\langle 01 | \rho(t) | 01 \rangle + \langle 10 | \rho(t) | 10 \rangle}, \quad (8)$$

as a function of time, number of CPMG cycles, and maximum coupling g_{max} . This normalization of $\langle \sigma_z \rangle$ eliminates the effect of T_1 noise in relevant cases (see Supplemental Material Sec. E [28]). We can compare the shapes of the measured decay envelopes with Eqs. (6) and (7), and the g dependence of decay rates with Eq. (4) to test the theory that our device is susceptible to Gaussian noise entering through the flux bias during two-qubit gates.

IV. EXPERIMENTAL RESULTS

As can be seen in Fig. 2(a), the experimentally measured Ramsey decay envelopes are well predicted by Gaussian $1/f$ noise. Additionally, as shown in Fig. 2(b), the scaling of the Gaussian decay rate with g_{max} agrees with the form of

Eq. (4). Notably, the decay rate increases by an order of magnitude as g_{\max} is increased from 10 to 50 MHz, suggesting that this coupler noise heavily exceeds single-qubit dephasing as an error mechanism during gates with large coupling, as predicted by Eq. (2). The flux sensitivity function extracted matches the theory well. From the data we extract a value of $\chi_{\phi}^{(2)}/\chi_{\phi}^{(1)} \cong 0.078$ ns, while a purely theoretical calculation using typical circuit parameters yields $\chi_{\phi}^{(2)}/\chi_{\phi}^{(1)} \cong 0.08$ ns. This excellent agreement with theory strongly suggests that noise during two-qubit gates is dominated by flux noise in the coupler, as hypothesized.

As predicted by Gaussian theory, the CPMG envelopes decay significantly slower than the Ramsey envelopes. However, as shown in Fig. 2, the details of these curves deviate from what would be predicted by Gaussian $1/f$ noise. While Eq. (7) predicts smooth decay, we see very clear steps in the decay curves. Additionally, the model predicts that the decay rate Γ_C should decrease proportionately to $\frac{1}{\sqrt{n}}$. This is not seen at all: The two curves “braid” and decay at the same rate.

The steps in the CPMG curves are difficult for any Gaussian noise model to produce (see Supplemental Material Sec. H [28] for further discussion on this). Therefore, these steps are signatures of non-Gaussian noise in our system. This non-Gaussian noise may be result of a small number of strongly coupled random telegraph noise (RTN) fluctuators [12], since Gaussian $1/f$ noise may be produced via a superposition of a large number of weakly coupled fluctuators [34] (see Supplemental Material Sec. B [28]). In the strong-coupling regime the Gaussian approximation for RTN may not be sufficient due to nonvanishing higher-order correlators in the cumulant expansion of the RTN decoherence function [12].

The CPMG decay curve associated with single RTN fluctuator with correlation time $t_c = \frac{1}{\gamma}$ is [35–37] (see Supplemental Material Sec. D [28])

$$\begin{aligned} \langle \sigma_z(t = 2mnt_g) \rangle &= \begin{cases} e^{-2mnyt_g} \left(q \frac{\cosh(n\alpha)}{\cosh(\alpha)} + \sinh(n\alpha) \right), & n \text{ odd,} \\ e^{-2mnyt_g} \left(q \frac{\sinh(n\alpha)}{\cosh(\alpha)} + \cosh(n\alpha) \right), & n \text{ even,} \end{cases} \end{aligned} \quad (9)$$

where

$$\begin{aligned} q &= -\frac{4\lambda^2}{\Omega^2} + \frac{\gamma^2 \cosh(2m\Omega t_g)}{\Omega^2}, \\ \sinh(\alpha) &= \frac{\gamma}{\Omega} \sinh(2m\Omega t_g), \end{aligned} \quad (10)$$

and $\Omega = \sqrt{\gamma^2 - 4\lambda^2}$, which may be real or imaginary, is the associated Rabi frequency.

We can validate this model by repeating the previous CPMG measurements for more values of n and attempting to fit the data simultaneously. The results of this are shown in Fig. 3. The decay envelopes are excellently described by a single, underdamped RTN fluctuator alongside single-qubit white-noise dephasing, which adds a simple exponential prefactor $e^{-\frac{\Gamma_{\phi}}{4}t}$ to Eq. (9) (see Supplemental Material Secs. E and F [28]). The scaling of fluctuator coupling strength with g is consistent with Eq. (5) (see Supplemental Material Sec. K [28]).

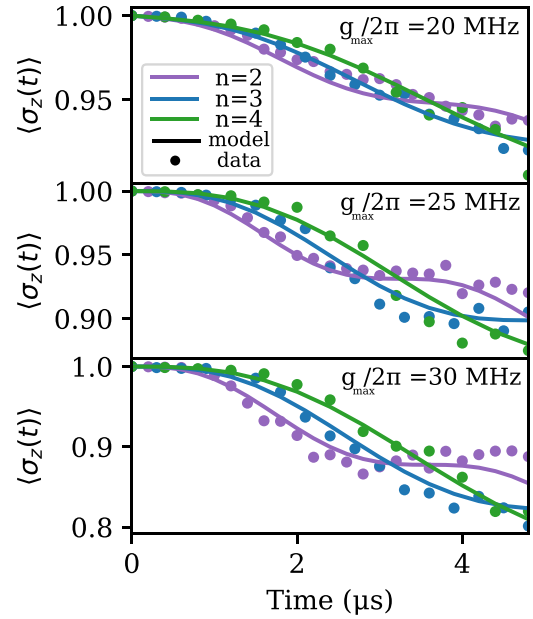


FIG. 3. Braiding in the CPMG decay envelopes. Fitting a single-fluctuator model to CPMG decay envelopes [Eq. (9)] for different values of n and g_{\max} . Each set of three curves is fit using only two parameters, γ and λ . Fits for more values of n can be found in Supplemental Material Sec. I [28]. Typical values of $t_c = \frac{1}{\gamma} \cong 50$ μs , $\frac{\lambda}{2\pi} \cong 0.1$ – 1 MHz (value depends strongly on g), and $\Gamma_{\phi}^{-1} \cong 100$ μs . All data points are the average of 10 000 samples.

In each case, the fit fluctuator is strongly in the underdamped regime, $2\lambda > \gamma$. In this regime (as shown in Supplemental Material Sec. J [28]), Eq. (9) is well approximated by

$$\langle \sigma_z(t = 2mnt_g) \rangle \cong e^{-2mnt_g\gamma} \left(1 + n \frac{\gamma}{\omega} \sin(2mt_g\bar{\omega}) \right), \quad (11)$$

where $\bar{\omega} = |\Omega|$. In this form, the dynamics are much more clear. The decay envelope will generally follow exponential decay and will produce steps with frequency $\frac{\bar{\omega}}{n}$. The implication of this is that it is difficult to dynamically suppress the decoherence caused by this kind of noise: More than $\frac{\bar{\omega}}{\gamma}$ echo pulses are required in time t to cause the trajectory to deviate significantly from exponential decay. This is significantly different than what would be expected for Gaussian $1/f$ noise for example, for which protection increases monotonically and smoothly with n .

Our results should not be confused with the well-known phenomenon of echo modulation observed in coupled spin systems. The latter would require simultaneous excitation of both qubits using single-qubit microwave pulses, while our technique relies on sequences of two-qubit gates enabled by a dc flux-bias control of the coupler frequency. As such, the dynamics is confined within a two-dimensional single-excitation subspace, i.e., our technique is mathematically equivalent to a dynamical decoupling of a single spin and the results should be interpreted within this framework.

V. CONCLUSION

It should be noted that this work alone is not enough to understand the physical origins of this non-Gaussian contri-

bution to the noise. Although this noise has been observed on several qubits in our system, this has not been studied systematically enough to determine if different qubits see fluctuators with similar parameters. Additionally, it would be impossible to tell if multiple pairs of qubits are seeing the same physical defect or just similar, independent defects with this kind of time-averaged, two-qubit measurement. These two situations may be discernible using time-averaged measurements taken after periodic pulse sequences on more than two qubits.

While the majority of this work was focused on the details of applying our technique to tunable-coupler transmons, the basic methods transfer readily to other qubit architectures. As an example from trapped ion quantum computing, a similar

technique could be used in the characterization of the effect of noise [38] on the coupling developed between ion electronic states during Mølmer-Sørensen gates [39].

ACKNOWLEDGMENTS

T.M. was supported in part by the U.S. Department of Energy, Office of Science, National Quantum Information Science Research Centers, Co-Design Center for Quantum Advantage under Contract No. DE-SC0012704. J.M. is partially supported by NAMS Contract No. NNA16BD14C. T.M. would like to thank John Chiaverini and John Martyn for their comments on the manuscript.

-
- [1] C. Neill, T. McCourt, X. Mi, Z. Jiang, M. Y. Niu, W. Mroczkiewicz, I. Aleiner, F. Arute, K. Arya, J. Atalaya *et al.*, *Nature (London)* **594**, 508 (2021).
- [2] F. Arute, K. Arya, R. Babbush, D. Bacon, J. C. Bardin, R. Barends, A. Bengtsson, S. Boixo, M. Broughton, B. B. Buckley, D. A. Buell, B. Burkett, N. Bushnell, Y. Chen, Z. Chen, Y.-A. Chen, B. Chiaro, R. Collins, S. J. Cotton, W. Courtney *et al.*, [arXiv:2010.07965](https://arxiv.org/abs/2010.07965).
- [3] A. T. K. Tan, S.-N. Sun, R. N. Tazhigulov, G. K.-L. Chan, and A. J. Minnich, *Phys. Rev. A* **107**, 032614 (2023).
- [4] F. Arute, K. Arya, R. Babbush, D. Bacon, J. C. Bardin, R. Barends, S. Boixo, M. Broughton, B. B. Buckley *et al.*, *Science* **369**, 1084 (2020).
- [5] J. Kelly, R. Barends, A. G. Fowler, A. Megrant, E. Jeffrey, T. C. White, D. Sank, J. Y. Mutus, B. Campbell, Y. Chen *et al.*, *Nature (London)* **519**, 66 (2015).
- [6] Z. Chen, K. J. Satzinger, J. Atalaya, A. N. Korotkov, A. Dunsworth, D. Sank, C. Quintana, M. McEwen, R. Barends, P. V. Klimov, S. Hong, C. Jones, A. Petukhov, D. Kafri, S. Demura, B. Burkett, C. Gidney, A. G. Fowler, H. Putterman, I. Aleiner *et al.*, *Nature (London)* **595**, 383 (2021).
- [7] F. Arute *et al.*, *Nature (London)* **574**, 505 (2019).
- [8] H.-Y. Huang, M. Broughton, J. Cotler, S. Chen, J. Li, M. Mohseni, H. Neven, R. Babbush, R. Kueng, J. Preskill, and J. R. McClean, *Science* **376**, 1182 (2021).
- [9] Y. Sung, L. Ding, J. Braumüller, A. Vepsäläinen, B. Kannan, M. Kjaergaard, A. Greene, G. O. Samach, C. McNally, D. Kim, A. Melville, B. M. Niedzielski, M. E. Schwartz, J. L. Yoder, T. P. Orlando, S. Gustavsson, and W. D. Oliver, *Phys. Rev. X* **11**, 021058 (2021).
- [10] B. Foxen, C. Neill, A. Dunsworth, P. Roushan, B. Chiaro, A. Megrant, J. Kelly, Z. Chen, K. Satzinger, R. Barends *et al.*, *Phys. Rev. Lett.* **125**, 120504 (2020).
- [11] G. S. Uhrig, *New J. Phys.* **10**, 083024 (2008).
- [12] Łukasz Cywiński, R. M. Lutchny, C. P. Nave, and S. Das Sarma, *Phys. Rev. B* **77**, 174509 (2008).
- [13] J. Bylander, S. Gustavsson, F. Yan, F. Yoshihara, K. Harrabi, G. Fitch, D. G. Cory, Y. Nakamura, J. S. Tsai, and W. D. Oliver, *Nat. Phys.* **7**, 565 (2011).
- [14] M. J. Biercuk, A. C. Doherty, and H. Uys, *J. Phys. B: At., Mol. Opt. Phys.* **44**, 154002 (2011).
- [15] X. You, A. A. Clerk, and J. Koch, *Phys. Rev. Res.* **3**, 013045 (2021).
- [16] L. M. Norris, G. A. Paz-Silva, and L. Viola, *Phys. Rev. Lett.* **116**, 150503 (2016).
- [17] Y. Sung, F. Beaudoin, L. M. Norris, F. Yan, D. K. Kim, J. Y. Qiu, U. von Lüpke, J. L. Yoder, T. P. Orlando, S. Gustavsson, L. Viola, and W. D. Oliver, *Nat. Commun.* **10**, 3715 (2019).
- [18] G. A. Paz-Silva, L. M. Norris, and L. Viola, *Phys. Rev. A* **95**, 022121 (2017).
- [19] P. Szańkowski, M. Trippenbach, and L. Cywiński, *Phys. Rev. A* **94**, 012109 (2016).
- [20] J. Krzywda, P. Szankowski, and L. Cywiński, *New J. Phys.* **21**, 043034 (2019).
- [21] A. G. Kofman and A. N. Korotkov, *Phys. Rev. A* **80**, 042103 (2009).
- [22] Y.-Q. Chen, K.-L. Ma, Y.-C. Zheng, J. Allcock, S. Zhang, and C.-Y. Hsieh, *Phys. Rev. Appl.* **13**, 034045 (2020).
- [23] M. A. Rol, F. Battistel, F. K. Malinowski, C. C. Bultink, B. M. Tarasinski, R. Vollmer, N. Haider, N. Muthusubramanian, A. Bruno, B. M. Terhal, and L. DiCarlo, *Phys. Rev. Lett.* **123**, 120502 (2019).
- [24] P. Dutta and P. M. Horn, *Rev. Mod. Phys.* **53**, 497 (1981).
- [25] R. J. Schoelkopf, P. Wahlgren, A. A. Kozhevnikov, P. Delsing, and D. E. Prober, *Science* **280**, 1238 (1998).
- [26] D. An, C. Matthiesen, E. Urban, and H. Häffner, *Phys. Rev. A* **100**, 063405 (2019).
- [27] F. Yoshihara, Y. Nakamura, F. Yan, S. Gustavsson, J. Bylander, W. D. Oliver, and J.-S. Tsai, *Phys. Rev. B* **89**, 020503(R) (2014).
- [28] See Supplemental Material at <http://link.aps.org/supplemental/10.1103/PhysRevA.107.052610> for additional calculations and experimental results that help support our findings.
- [29] F. Yan, P. Krantz, Y. Sung, M. Kjaergaard, D. L. Campbell, T. P. Orlando, S. Gustavsson, and W. D. Oliver, *Phys. Rev. Appl.* **10**, 054062 (2018).
- [30] R. Koch, J. Clarke, W. Goubau, J. Martinis, C. Pegrum, and D. van Harlingen, *J. Low Temp. Phys.* **51**, 207 (1983).
- [31] E. L. Hahn, *Phys. Rev.* **80**, 580 (1950).
- [32] H. Y. Carr and E. M. Purcell, *Phys. Rev.* **94**, 630 (1954).
- [33] S. Meiboom and D. Gill, *Rev. Sci. Instrum.* **29**, 688 (1958).
- [34] F. Hooge, *IEEE Trans. Electron Devices* **41**, 1926 (1994).
- [35] G. Ramon, *Phys. Rev. B* **92**, 155422 (2015).
- [36] Y. M. Galperin, B. L. Altshuler, J. Bergli, and D. V. Shantsev, *Phys. Rev. Lett.* **96**, 097009 (2006).
- [37] L. Faoro and L. Viola, *Phys. Rev. Lett.* **92**, 117905 (2004).
- [38] D. Hayes, S. M. Clark, S. Debnath, D. Hucul, I. V. Inlek, K. W. Lee, Q. Quraishi, and C. Monroe, *Phys. Rev. Lett.* **109**, 020503 (2012).
- [39] K. Mølmer and A. Sørensen, *Phys. Rev. Lett.* **82**, 1835 (1999).